Modelling the effect of atomic transitions on the relationship between attenuation coefficients and nuclear g-factor

Justin Lee (u6150650)

November 4, 2019

Abstract

The Recoil-in-Vacuum method is a potentially useful tool in measuring the g-factor of nuclei, but the correlation between the attenuation factor measured by this method and the g-factor is not entirely clear. This project aims to code a Monte-Carlo simulation to better understand this correlation. We find that the suspected g^2 correlation indeed holds in the limit of weak hyperfine fields and short atomic lifetimes, while the currently used $|g|$ correlation is a better fit otherwise.

Introduction

1.1 The Recoil in Vacuum (RIV) method

The measurement of the g-factor of a nucleus is of great interest as it provides insights into how the nucleus carries its angular momentum [1, p. 30], and this is often done by measuring the hyperfine structure of an atom or ion containing that nucleus. One way to do this is via the Recoil-in-Vacuum method, where a beam of the ions of interest is fired at a target (such as a carbon foil), electromagnetically exciting the ions as they recoil into the vacuum.

This excitation (usually a Coulomb excitation) fixes the initial orientation of the nuclear spins of the ions relative to the beam axis while the electron spins remain randomly oriented. After this excitation the ions recoil into the vacuum, allowing hyperfine interactions (i.e. the coupling between the nuclear magnetic moment and the field generated by the electron configuration) as in fig. 1) to take over.

The effect of the hyperfine interaction is periodic in nature and can be described by the precession frequency $\omega_{FF'}$, which is given as [1, p. 33]

$$\omega_{FF'} = \frac{A_J}{2\hbar}[F(F+1) - F'(F'+1)], \qquad (1)$$

where the hyperfine interaction constant A_J is

$$A_J = \frac{g\mu_N B}{J} \qquad (2)$$

where g is the g-factor, μ_N is the nuclear magneton, B is the hyperfine magnetic field at the nucleus and J is the angular momentum of the electronic configuration.

As the nuclei ions are excited, a clever way of measuring this coupling interaction is by looking at the angle of the gamma ray emissions as the nuclei undergo decay. The emitted gamma rays vary in intensity as a function of angle in

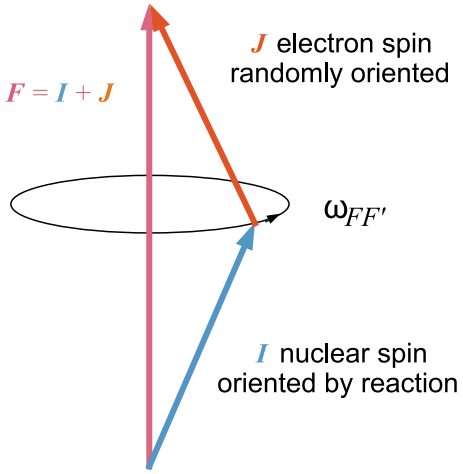

Figure 1: Schematic of the hyperfine coupling [1, p. 31]

a 'clover' shape (fig. 2), and they are dependent on the nuclear spin. Indeed, we can write this angular correlation of gamma ray intensity, $W(\theta)$ (where θ is the angle of gamma ray emission relative to the beam axis), as a multipole expansion [2, p. 220]:

$$\begin{aligned} W(\theta,t) =& 1 + G_2(t)Q_2 \cdot A_2 \cdot P_2 \cos\theta \\ &+ G_4(t)Q_4 \cdot A_4 \cdot P_4 \cos\theta, \end{aligned} \tag{3}$$

where Q_k are the solid-angle corrections, P_k are Legendre polynomials of degree $k = 2, 4$, A_k are the unperturbed angular correlation parameters, and G_k are the attenuation coefficients.

Unperturbed angular correlation in this case means the W observed when the hyperfine interactions are observed immediately upon excitation (i.e. before any vacuum deorientation takes place). While this immediate decay cannot be measured directly, the unperturbed correlation can be measured by implanting the ions into a medium like copper (see top left diagram of fig. 2). The anisotropy seen in this unperturbed W is reduced when the hyperfine interactions are allowed to occur in the vacuum. G_k can then be thought of as a factor describing this attenuation of the anisotropy of W, with the unperturbed anisotropy of W having a G_k value of 1, and all perturbed G_k having values between 0 and 1.

1.2 The attenuation factor, G_k

In real experiments, $G_k(t)$ can be measured using a plunger mechanism [3, p. 1]. A beam of ions is excited in a target foil and stopped in a stopper at a set distance from the target. Once the ions hit the stopper, the hyperfine interactions are quenched, fixing the nuclear spin in place and the nucleus is left to decay. As the ions travel at a fixed and known velocity, the target-to-stopper distance can be treated as a function of t, as the gamma rays that are emitted at the stopper correlate with the nuclear spin orientations at t. Note that it is possible for the ions to undergo nuclear decay before reaching the stopper, but this can be detected and accounted for due to Doppler shifting [2, p. 221].

Assuming the electron spins are initially randomly oriented, we get the following equation for $G_k(t)$ [4, p. 84]:

$$\begin{aligned} G_k(t) = \sum_{F,F'} \frac{(2F+1)(2F'+1)}{2J+1} \begin{Bmatrix} F & F' & k \\ I & I & J \end{Bmatrix}^2 \\ \times \cos(\omega_{FF'}t), \end{aligned} \tag{4}$$

where I is the nuclear spin, J is the atomic spin, F and F' are the possible couplings of I and J from $\mathbf{F} = \mathbf{I} + \mathbf{J}$. The expression with the curly brackets is the Wigner $6j$-symbol.

It is the relationship between G_k and g that is of great interest, as knowing this possibly al-

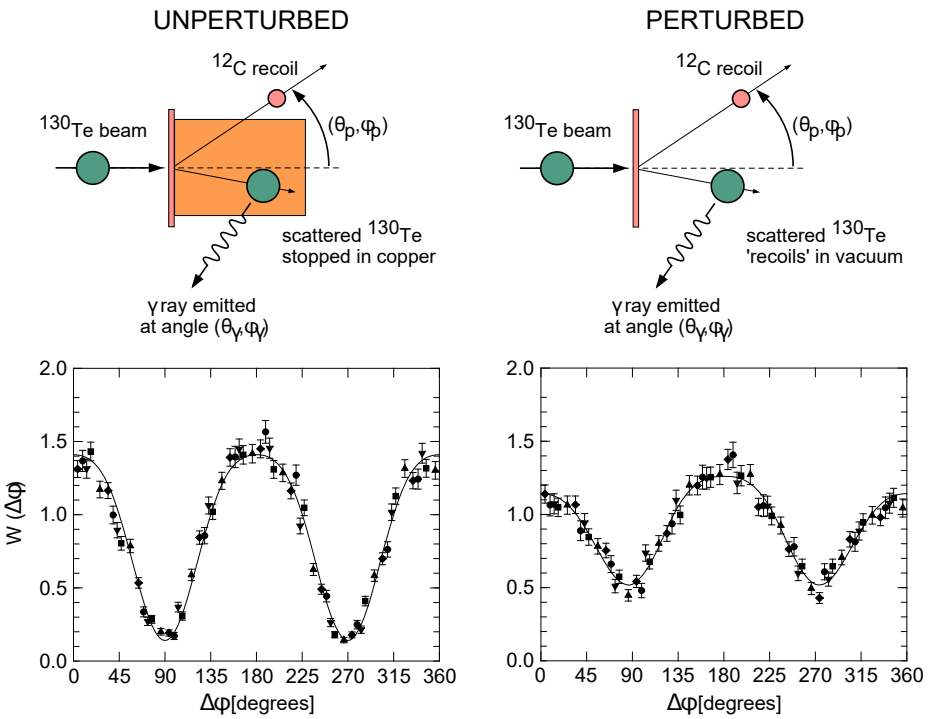

Figure 2: *Left:* Unperturbed angular correlations for the $2_1^+ \to 0_1^+$ transition following implantation in ^{130}Te into copper *Right:* Perturbed angular correlations for the same transition after allowing the ion to travel through vacuum [1, p. 32]

lows for reliable measurements of the g-factor using the RIV technique.

In the absence of atomic decays in the vacuum where the electrons spontaneously emit photons and lose energy (a process known as atomic decay, analogous to the gamma decay mechanism for the nuclei except it is the electrons losing energy, and the photons emitted are less energetic than gamma photons) and when all ions start off (and remain) in the same atomic state, $G_k(t)$ exhibits simple periodicity due to the $\cos(w_{FF'}t)$ term in eq. (4). But if we account for different distributions of atomic states and possibly atomic decay, we get a quasi-exponential or exponential decay. The exact type of decay depends on the way the atomic decay takes place.

The general physical intuition behind this decay can be thought of as a combination of decoherence and information loss. The electron and nuclear spins are precessing with a frequency $\omega_{FF'}$, and initially the nuclear spins are oriented the same way for every ion. The distribution of the electron spins is random, however, and so the electron and nuclear spins precess about the different directions of F, which varies with the direction of J. Despite this difference in precession axis, if all of the ions share the same electron spin state (but not necessarily orientation), then by eq. (1) they should all point in the same direction after every period, returning W to its maximum anisotropy. This gives the periodic oscillation of $G_k(t)$.

Generally, the ions recoiling into vacuum will have a range of charge states and thus be excited into various electronic states, thus there will be a distribution of atomic spins J and hyperfine fields B, thus giving a distribution of precession frequencies $\omega_{FF'}$. Once we account for this distribution decoherence starts to appear. Even though information is not lost as the nuclear spins do go back to the original orientation after each period, they do not all share the same period. This gives a quasi-exponential decay of $G_k(t)$ that can be decomposed into periodic $G_k(t)$ of the possible

atomic spin states for the ions.

With atomic decay, the spins precess about a new axis based on the orientation of the nuclear spin at the time the atomic decay occurred. This means the ion has 'forgotten' the nuclear spin the previous state started off with. Thus with each atomic decay the nuclear spin's orientation after each period would resemble the original nuclear spin orientation less. This is true information loss as it is not possible to recover the previous spin orientations from a $G_k(t)$ curve at the end of this process.

1.3 The g-factor correlation

A static model in the context of RIV refers to a model that does not account for atomic decays. Rather, the average is taken for the G_k values of various atomic states that remain fixed throughout time. As mentioned before, this gives a quasi-exponential distribution. However, when the distribution of the hyperfine magnetic fields B is taken to be a Lorentzian distribution, it can be shown analytically that the decay is exponential, with a decay constant proportional to $|g|$ [1, p. 37].

On the other hand, if we allow for atomic decays with a fluctuating model, under a distribution of fields the Abragam-Pound theory states that G_k would undergo an exponential decay with a decay constant proportional to g^2 [2, p. 222].

It is generally believed that the static model is sufficient for analysis, with Stuchbery and Stone concluding in 2007 that for Te ions, there are not enough atomic transitions up to around 10 ps to have much of an impact [5]. Thus the decay constant has usually been taken to be proportional to $|g|$.

However, more recent results (fig. 3) from an RIV experiment conducted in the Australian National University with Ge and Se ions have called this conclusion into question. When plotted against $g\tau$, where τ is the atomic lifetime (the mean time it takes for the ion to undergo atomic decay) the G_k curves seem to be different, suggesting different atomic structures between Ge and Se ions as the g-factors have been measured independently [6]. This is unexpected given that the hyperfine structure of Ge and Se ions were expected to be mostly the same.

This difference mostly disappears if G_k is plotted against $g^2\tau$, and if the exponential decay is indeed correlated with g^2, then the hyperfine fields can be inferred to be mostly the same for Ge and Se. This has revived interest in a g^2 correlation for the exponential decay.

Analytically, it should not be surprising that a g^2 correlation should result for small atomic lifetimes when we take into account atomic decay as in the fluctuating model. Consider the Maclaurin expansion of the $\cos(\omega_{FF'}t)$ term in eq. (4):

$$\cos(\omega_{FF'}t) \approx 1 - \frac{(\omega_{FF'}t)^2}{2}, \qquad (5)$$

so for small enough $\omega_{FF'}t$, $G_k(t)$ would primarily be a function of $(\omega_{FF'}t)^2$. Keeping in mind eqs. (1) and (2), we can see that $G_k(t)$ should be a function of g^2 as well.

Finding the exact $\omega_{FF'}t$ values at which this expansion is valid and additionally leads to an exponential decay is not so trivial. Additionally, this does not tell us about the characteristics of $G_k(t)$ as it approaches this limit. For these, a simple Monte-Carlo simulation of the mathematical assumptions behind this fluctuating model could prove useful. Full atomic physics calculations are being developed separately and are outside the scope of this project.

Methods

2.1 Assumptions for the model

When creating a Monte-Carlo simulation, some simplifications have to be made with certain assumptions.

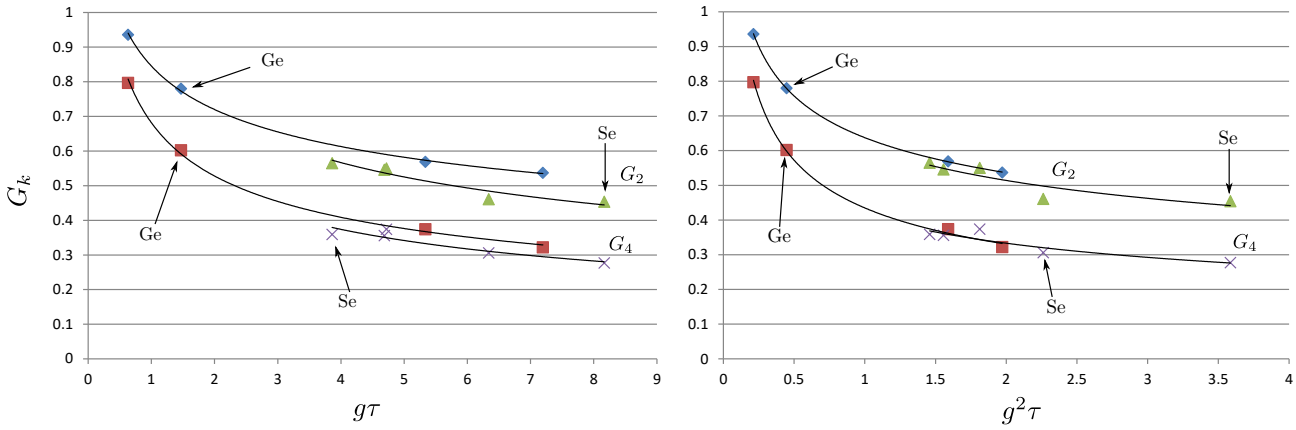

Figure 3: G_k curves of Ge and Se ions of various isotopes fired from a carbon foil at a velocity of $\frac{v}{c} \approx 4.6\%$. *Left:* G_k values plotted against $g\tau$. *Right:* G_k values plotted against $g^2\tau$

1 The distribution of atomic spins is isotropic

Although this is not necessarily the case (but is believed to be a good assumption nonetheless), we can only use eq. (4) by assuming the electron spins are initially randomly oriented. Had we not assumed this, we would need to work out G_k from the tensor of the coupled system at each individual time t [1, p. 33].

2 Only $E1$ photons are emitted from atomic decay

Although higher multipole transitions are possible, $E1$ transitions which can only carry away $1\hbar$ of spin dominate atomic decay mechanisms especially on smaller timescales. Electron spin is equally likely to go up or down a level or remain the same with each decay.

3 The hyperfine magnetic field B is Lorentz distributed around $B = 0\text{T}$

Although a Gaussian distribution of hyperfine fields might be closer to reality, the analysis showing an exponential decay of $G_k(t)$ as well as its g^2 dependence was done for Lorentz distributed B as they were easier to work with mathematically [2, p. 224].

4 The nucleus does not decay in flight

As in-flight nuclear decay is accounted and adjusted for in real experiments, there is no need to model this phenomenon within the scope of this project, as there should not be any real difference in the results of the measurement. In fact, in-flight nuclear decays can be filtered out in real life measurements without changing the result.

2.2 Algorithm of the Monte-Carlo simulation

The Monte-Carlo simulation was coded in Python.

Before the simulation begins, F and F' are computed for all possible combinations of I and J values, where $\min(F) = \min(F') = |I - J|$, $\max(F) = \max(F') = |I + J|$, and the F and F' values in-between are separated by 1. So for example, for $I = 2$ and $J = 1.5$, the possible values of F and F' are 0.5, 1.5, 2.5, and 3.5.

In the first step, a particle starts off with $G_k(0) = 1$ at $t = 0$ with a random atomic state quantum number J chosen from a uniform distribution of allowed atomic states.

In the second step, a random atomic survival time t_{ai} (i.e. how long the particle remains in this atomic state before atomic decay) is gen-

erated, weighted according to the atomic lifetime τ by $e^{-t_{ai}/\tau}$ (i.e. the atomic lifetime is the mean atomic survival time). This step is repeated from $i = 1$ until $i = n$ where $\sum_{i=1}^{n} t_{ai}$ exceeds the relevant final time t_f we want to compute for. t_{an} is then subtracted with $\sum_{i=1}^{n} t_{ai} - t_f$ so that the new $\sum_{i=1}^{n} t_{ai} = t_f$. The atomic decay is simulated with every new atomic lifetime generated by having J increase or decrease by 1 and this sequence of J is stored for subsequent steps alongside the t_{ai} values.

In the third step, for each i eq. (4) is used to compute $G_k(t_{ai})$ with their respective J values and then multiplied with the $G_k(t_{ai})$ before it, and for t_{a1}, $G_k(t_{a1})$ is multiplied with $G_k(0)$. This is to simulate the information loss arising from atomic decay as mentioned in the previous section. The hyperfine fields B in this calculation are also randomly determined every transition by a Lorentz distribution multiplied by a factor.

In the fourth step, $G_k(t)$ is calculated for each t we want to sample on. This is done by finding the largest t_{ai} value less than t, computing $G_k(t - t_{ai})$ with the J value associated with said t_{ai} and finally multiplying $G_k(t-t_{ai})$ with $G_k(t_{ai})$. The number of atomic decays elapsed from $t = 0$ to the sampled t is also recorded.

All four steps are repeated for as many trials as needed, with 10,000 trials being a good number for producing consistent statistics within a reasonable time.

2.3 Parameters

The following parameters can be adjusted in the simulation:

- k value of G_k
- The nuclear spin state I that remains constant throughout the simulation
- Range of allowed atomic states J
- Initial and final times to plot $G_k(t)$ over, where $t = t_f$ is the final time
- Factor to multiply Lorentz distributed B values by (hereafter referred to as η)
- Atomic lifetime, τ
- g-factor, g

Throughout the simulation, $I = 2$ and J has the allowed values 0.5, 1.5, and 2.5. We can then vary τ and g. For this paper, we stepped g from 0.2 to 2.0 in 0.2 steps for $\tau = \{0.5, 1.0, 2.0, 3.0, 4.0, 5.0, 6.0, 7.0,$
$8.0, 9.0, 10.0, 15.0, 30.0\}$ ps. Various η values (chosen to reflect realistic B values from Hartree-Fock calculations) were also tested.

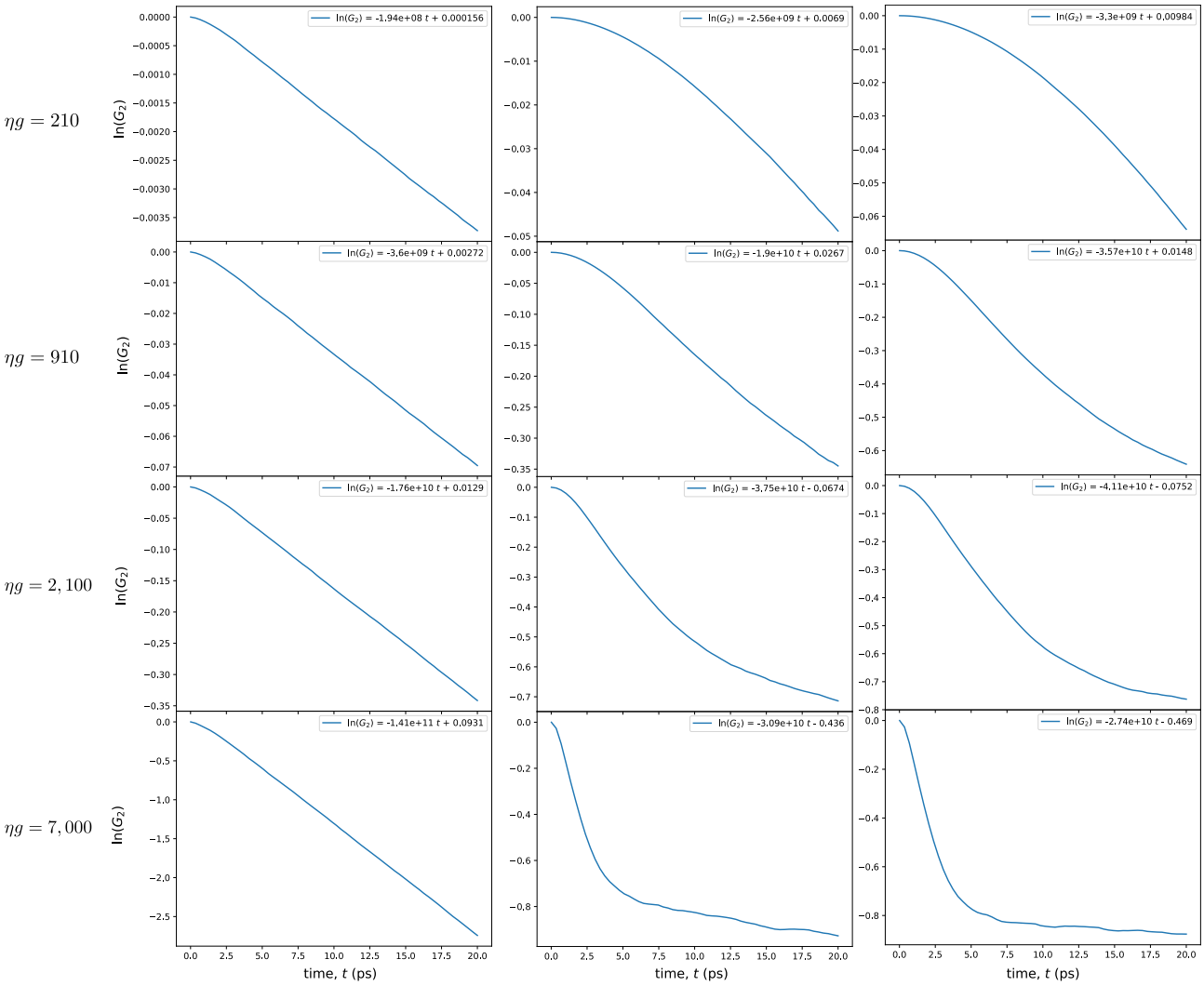

Figure 4: Log-linear plots of $G_2(t)$ for combinations of various parameters of ηg and τ plotted over $t \in [0.01, 20]$ ps. The top right equation on each plot is the the best log fit curve through $G_2(t)$ for the respective graphs. The graphs increase in ηg from 210 through 7,000 from top to bottom, and the atomic lifetime τ increases from left to right.

Results & Discussion

3.1 Exponential decay

For this, ηg will be used for comparison as B and g are coefficients of each other in eq. (2) and they appear nowhere else in the calculations, thus changing either of them should yield the same effect.

Plots were taken for fig. 4 from $t = 0.01$ ps to $t = 20.0$ ps. For small values of τ, we find that the $G_k(t)$ undergoes almost perfect exponential decay , except at very small t. All of the graphs exhibit a non-exponential decay at very small t, this can be accounted for by noting that at these t values it is very unlikely for any of the ions to undergo the first decay, so $G_k(t)$ is mostly dominated by a superposition of periodic functions very briefly in the beginning. This conclusion is further supported by noting that this 'flat' beginning is longer when τ is longer as well.

For larger τ values, however, there is apparently a 'sweet spot' located around $\eta g = 910$ where the exponential decay mostly holds even for relatively large τ, where few atomic transitions occur.

As η increases, G_k decays at a faster rate. It is also interesting to note that the exponential decay breaks in different ways when η is very small or very large. At lower η values the $\ln(G_k(t))$ plot begins to look more 'convex', while at larger η values the $\ln(G_k(t))$ takes on a more 'concave' shape, even looking like it is splitting into two separate exponential decays. The second exponential decay (the 'lower arm') occurs at a much slower rate, creating a 'floor' for $G_k(t)$.

The convexity for small η can simply be explained by looking at the expansion in eq. (5) again. $G_k(t)$ simply behaves like a quadratic equation here, and indeed if we plot $\sqrt{1 - G_k(t)}$ against t we get a linear correlation:

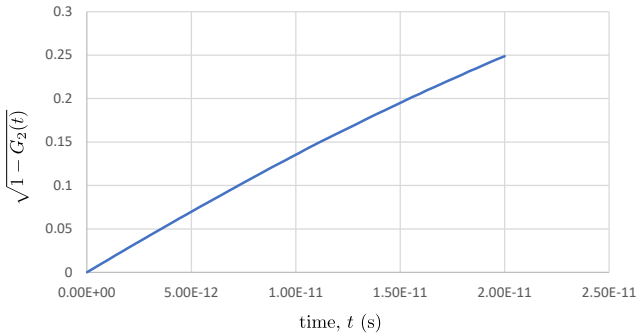

Figure 5: Plot of $\sqrt{1 - G_2(t)}$ against t for $\eta g = 210, \tau = 100$ ps

The concavity is not as easily explained, however. The 'elbows' of the curves occur at the same t even at different τ (e.g. in the case of $g = 1.4$ it is at $t \approx 5$ ps for $\eta g = 7,000$ at $\tau = 30.0, 100.0$). Higher τ values cause a sharper elbow and shift the elbow upward, while increasing ηg shifts the elbow to the left. The vertical position of the elbow seems independent of ηg.

ηg	approx. t of 'elbow' (ps)
910	31
2,100	17
4,200	6.9
7,000	5.0
8,400	4.4
11,200	3.3
12,600	2.9
14,000	2.5
21,000	2.0
28,000	1.3

Table 1: Variation of horizontal 'elbow' position of $\ln(G_2(t))$ plot for various ηg taken at $\tau = 100$ ps.

()

τ (ps)	approx. t of 'elbow' (ps)	approx. $G_k(t)$ of 'elbow'
5	2.6	0.64
10	3.6	0.60
20	6.4	0.50
50	7.0	0.46
100	6.7	0.47
200	8.0	0.45

Table 2: Variation of vertical 'elbow' position of $\ln(G_2(t))$ plot for various ηg taken at $\eta g = 7,000$.

From table 1, the 'elbow' that seemed absent in fig. 4 in the case of $\eta g = 910$ is actually there, it has just been shifted to the right past $t = 20$ ps: The 'sweet spot' is actually dependent on the t interval of interest.

The leftwards elbow shift with increasing ηg (which in turn increases $\omega_{FF'}$) might be due to the 'speeding up' of decoherence from increased precession speed. Increasing τ (and thus decreasing the number of atomic decays in the same amount of time) shifts the elbow to the *right* and also moves the elbow downwards, at least up to a limit where an increase in τ does not move the elbow down further, only leftwards.

This difference in behaviour when varying ηg and when varying τ points to the inherent differences in the way they affect attenuation. Recall that the decoherence from precession alone does not actually result in information loss, so increasing the precession speed should not result in more information loss, only that the attenuation should reach the minimum (the lower arm) faster. Conversely, increasing the number of atomic decays within the same time interval (by decreasing τ) not only speeds up the decrease of $G_k(t)$ towards the minimum, but this increased information loss prevents the orientation of the spins from 'recovering' as much, thus lowering the minimum $G_k(t)$ until it reaches the point where maximum deorientation is reached.

As the slope of the upper arm of $\ln(G_k(t))$ clearly depends on ηg and τ in different ways, the investigation of the g-factor correlation on G_k needs to take these variations into account.

3.2 g-factor correlation of $G_k(t)$

The 'upper arm' of $\ln(G_k(t))$ is an exponential decay that can be written as

$$G_k(t) = Ae^{-\Gamma t}, \tag{6}$$

where A is some constant and $-\Gamma$ is the decay constant, and we can rewrite this in terms of $\ln(G_k(t))$:

$$ln(G_k(t)) = -\Gamma t + B, \tag{7}$$

where B is some constant and $-\Gamma$ here is the slope of the upper arm of $\ln(G_k(t))$.

If Γ is proportional to $|g|$, then it should be the case that

$$C|g| = \Gamma, \tag{8}$$

where C is constant for all g (but not necessarily constant for all *eta* or τ).

On the other hand, if Γ is proportional to g^2, then it should be the case that

$$Cg^2 = \Gamma. \tag{9}$$

To see if a $|g|$ or g^2 correlation is better, we took $C = \Gamma/g^{\mathrm{n}}$ for $\mathrm{n} = 1, 2$ and observed how invariant they were to various g values. The more horizontal the lines, the better.

small ηg, small τ

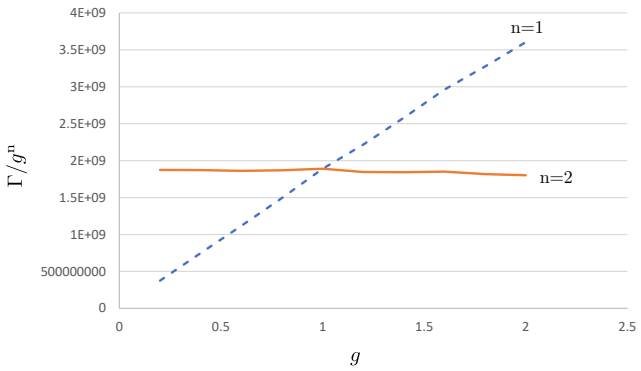

Figure 6: Γ/g^{n} vs g for $\eta = 650$, $\tau = 0.5$ ps

small ηg, large τ

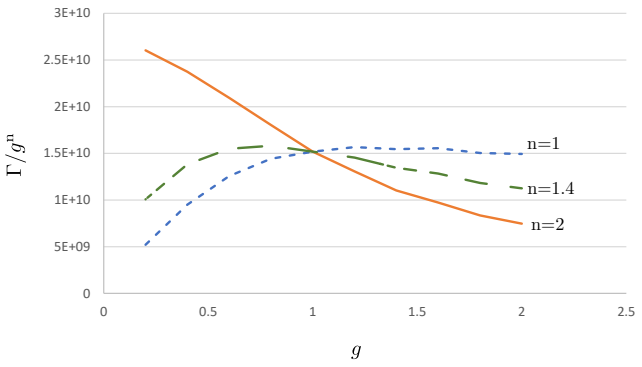

Figure 7: Γ/g^n vs g for $\eta = 650$, $\tau = 30.0$ ps

large ηg, small τ

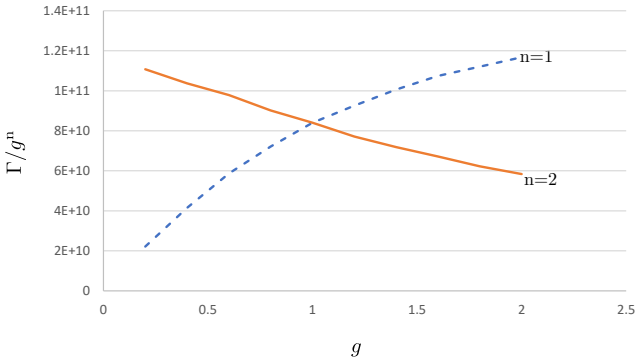

Figure 8: Γ/g^n vs g for $\eta = 5{,}000$, $\tau = 0.5$ ps

large ηg, large τ

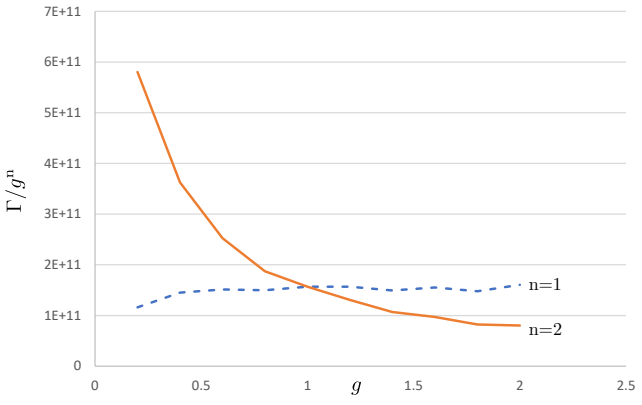

Figure 9: Γ/g^n vs g for $\eta = 5{,}000$, $\tau = 30.0$ ps

For small ηg and τ values such as $\eta = 650$ and $\tau = 0.5$ ps (fig. 6), Γ/g^2 remained largely constant, indicating a g^2 correlation in this regime. As τ becomes large, however, the $|g|$ fit becomes a better approximation (although still not a good one). In the case of $\eta = 650, \tau = 30.0$ ps, $n = 1.4$ was actually found to be the best fit (see fig. 7) but it still does not fit as well as g^2 did in the small τ limit. It should be noted that Γ is less accurate here as $\ln(G_k(t))$ exhibits the convexity found in the upper right plots in fig. 4.

With large ηg and small τ (fig. 8), both $|g|$ and g^2 fits are equally accurate. But as τ gets larger in this case (fig. 9), g^2 decay becomes a very poor fit while $|g|$ remains reasonable.

These results agree with the theory. Larger η values mean larger $\omega_{FF'}$ and larger τ values mean longer interaction times, thus the Maclaurin expansion of $\cos(\omega_{FF'}t)$ from eq. (5) becomes less accurate in either case, and if both are the case then the accuracy drops further. i.e. the g^2 approximation works best when both τ and ηg are small.

3.2.1 Locating the transition between $|g|$ and g^2 correlations

Finally, it might be useful to try to locate where this transition occurs.

For this example, $\eta = 650$. We plotted the variance of Γ/g and Γ/g^2 divided by Γ over $g \in [0.2, 2.0]$ with $\Delta g = 0.2$ steps for various τ:

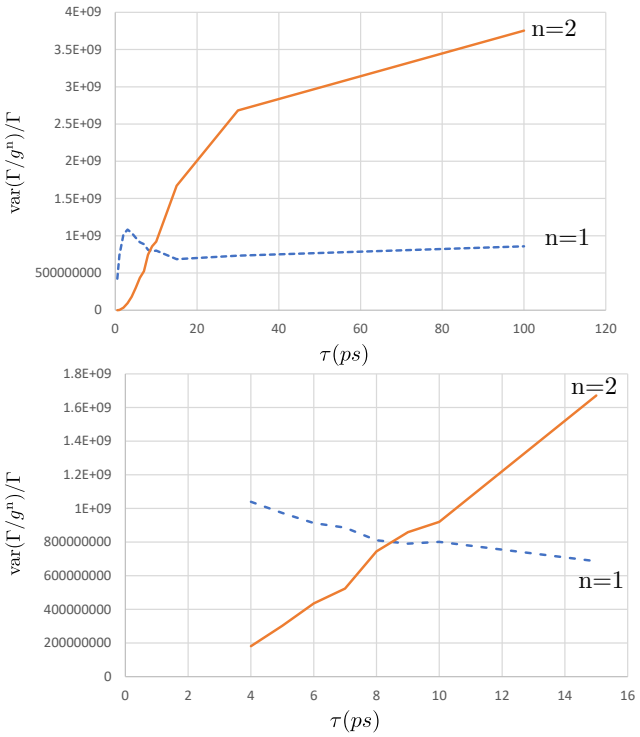

Figure 10: Plot of $\text{var}(\Gamma/g^{\text{n}})/\Gamma$ against $\tau = 0.5, 1, 2, 3, 4, 5, 6, 7, 8, 9, 10, 15, 30, 100$ ps and $\eta = 650$. *Top:* Plot over an interval $\tau \in [0.5, 100]$ ps *Bottom:* The same plot over an interval $\tau \in [4, 15]$ ps.

Here, larger $\text{var}(\Gamma/g^{\text{n}})/\Gamma$ values denote larger variance: Smaller $\text{var}(\Gamma/g^{\text{n}})/\Gamma$ values indicate a more constant Γ/g^{n} for the relevant τ and hence a better fit.

We can see that the $|g|$ fit remains largely consistent throughout except at small τ, where g^2 provides a remarkably accurate fit. The g^2 correlation rapidly degrades until slightly past $\tau = 8$ ps, where the $|g|$ correlation more accurately describes $G_k(t)$. This might explain the $|g|$ correlation observed with certain ions.

It might be helpful and more intuitive to put this in terms of the number of atomic decays. At $\tau = 8$ ps, an average of 1.3 atomic decays would have occurred by $t = 10$ ps, and 2.5 atomic decays by $t = 20$ ps. At $\tau = 0.5$ ps, an average of 20.3 atomic decays would have occurred by $t = 10$ ps, and 40.0 atomic decays by $t = 20$ ps.

Thus if we are analysing ions that have a hyperfine field distributed around $B = 650$ T, they need to have more than an average of 1.27 atomic decays by 10 ps for the g^2 correlation to appear, with more atomic decays giving a stronger g^2 correlation.

Although the analysis was for G_2, all of it holds for G_4. Indeed, the only difference in calculation between G_2 and G_4 lies in the wigner function and not in $\omega_{FF'}$ in eq. (4), which can just be treated as a constant coefficient to $\cos(\omega_{FF'}t)$.

Conclusion

This Monte-Carlo simulation of the fluctuating model not only confirms the g^2 correlation for ions with small atomic lifetimes and weak hyperfine fields, but it allowed us to approximately locate where this g^2 correlation disappears to give the current $|g|$ correlation found in recent literature for the RIV technique.

In addition, with the help of the simulation this project has demonstrated how the exponential decay breaks down.

Further investigation using more complete atomic simulations can be done to confirm these results and narrow down the point where the g^2 correlation becomes reasonably strong.

References

[1] A. E. Stuchbery, "Free-ion hyperfine fields and magnetic-moment measurements on radioactive beams: Progress and outlook," *Hyperfine Interactions*, vol. 220, no. 1-3, pp. 29–45, Nov. 2012. DOI: 10.1007/s10751-012-0683-7. [Online]. Available: https://doi.org/10.1007/s10751-012-0683-7.

[2] R. Brenn, H. Spehl, A. Weckherlin, H. A. Doubt, and G. van Middelkoop, "Nuclear deorientation for heavy ions recoiling in vacuum and low pressure gas," *Zeitschrift für Physik A Atoms and Nuclei*, vol. 281, no. 3, pp. 219–227, Sep. 1977, ISSN: 0939-7922. DOI: 10.1007/BF01408840. [Online]. Available: https://doi.org/10.1007/BF01408840.

[3] X. Chen, D. G. Sarantites, W. Reviol, and J. Snyder, "Time-dependent Monte Carlo calculations of recoil-in-vacuum g-factor data for ^{122,126,130,132}Te," *Phys. Rev. C*, vol. 87, p. 044 305, 4 Apr. 2013. DOI: 10.1103/PhysRevC.87.044305. [Online]. Available: https://link.aps.org/doi/10.1103/PhysRevC.87.044305.

[4] M. Blume, "Perturbed angular correlations: Perturbation factor for arbitrary correlation time," *Nuclear Physics A*, vol. 167, no. 1, pp. 81–86, May 1971. DOI: 10.1016/0375-9474(71)90583-5. [Online]. Available: https://doi.org/10.1016/0375-9474(71)90583-5.

[5] A. E. Stuchbery and N. J. Stone, "Recoil in vacuum for te ions: Calibration, models, and applications to radioactive-beam g-factor measurements," *Phys. Rev. C*, vol. 76, p. 034 307, 3 Sep. 2007. DOI: 10.1103/PhysRevC.76.034307. [Online]. Available: https://link.aps.org/doi/10.1103/PhysRevC.76.034307.

[6] B. P. McCormick, A. E. Stuchbery, B. A. Brown, G. Georgiev, B. J. Coombes, T. J. Gray, M. S. M. Gerathy, G. J. Lane, T. Kibédi, A. J. Mitchell, M. W. Reed, A. Akber, L. J. Bignell, J. T. H. Dowie, T. K. Eriksen, S. Hota, N. Palalani, and T. Tornyi, "First-excited state g factors in the stable, even Ge and Se isotopes," *Phys. Rev. C*, vol. 100, p. 044 317, 4 Oct. 2019. DOI: 10.1103/PhysRevC.100.044317. [Online]. Available: https://link.aps.org/doi/10.1103/PhysRevC.100.044317.